Coordination Chemistry Hot Paper

How to cite: *Angew. Chem. Int. Ed.* **2021**, *60*, 14179–14187
International Edition: doi.org/10.1002/anie.202103755
German Edition: doi.org/10.1002/ange.202103755

Reduced Arene Complexes of Hafnium Supported by a Triamidoamine Ligand

Priyabrata Ghana, Sebastian Schrader, Thayalan Rajeshkumar, Thomas P. Spaniol, Ulli Englert, Laurent Maron, and Jun Okuda**

Abstract: *A series of hafnium complexes with a reduced arene of the general formula [K(L)][Hf(Xy-N_3N)(arene)] (Xy-N_3N = {(3,5-$Me_2C_6H_3$)NCH_2CH_2}$_3N^{3-}$, L = THF, 18-crown-6; arene = $C_{10}H_8^{2-}$, $C_{14}H_{10}^{2-}$) mimic the chemistry of hafnium in its formal oxidation state +II. All compounds were obtained upon reduction of the chlorido complex [HfCl(Xy-N_3N)(thf)] with two equivalents of potassium naphthalenide or anthracenide. The reducing nature and the basicity of the reduced anthracene ligand were explored in the reaction of benzonitrile and azobenzene, and by deprotonation of tert-butylacetylene, respectively. The reduction of benzonitrile provides an initial double nitrile insertion product under kinetic control that rearranges after extrusion of one of the inserted nitriles to a hafnium imido complex as the thermodynamic product. The reduction of azobenzene resulted in a diphenylhydrazido(2−) complex. Treatment of terminal alkynes with the anthracene or diphenylhydrazido(2−) complex led to the selective protonation of the corresponding dianionic ligand.*

Introduction

Metal complexes of reduced, polycyclic arene ligands constitute a special class of organometallic reagents that serves as soluble metal reductants owing to the lability of the arene ligands during reduction.[1] The most common examples are alkali or alkaline earth metal naphthalenides and anthracenides.[2,3] Recently, considerable interest was also shown towards the synthesis of reduced arene complexes of transition metals, driven by their potential use as a storable source of low-valent transition metals.[4] For example, the iron(II) reduced naphthalene complex [K(18-crown-6)][Cp*Fe(η^4-$C_{10}H_8$)] (Cp* = C_5Me_5) acts as a convenient "Cp*Fe$^-$" source in the activation of white phosphorus, where it mimics the chemistry of a formal Fe^0 complex.[5] While a variety of reduced arene complexes were isolated for titanium[6] and zirconium,[7] corresponding complexes for the heavier congener hafnium are limited to their homoleptic homologue $[K(18\text{-crown-6})]_2[Hf(arene)_3]$ (arene = $C_{10}H_8^{2-}$, $C_{14}H_{10}^{2-}$, cyclooctatetraenide ($C_8H_8^{2-}$)).[8] These tris-(arene)hafnates with a formally Hf^{2-} center were proposed as suitable precursors for studies on poorly explored low-valent hafnium chemistry. So far only five complexes of hafnium in the formal oxidation state of +II have been isolated, for example $[Cp_2Hf(CO)_2]$, $[CpHf(dmpe)Cl(CO)_2]$, $[Hf_2I_4(PMe_2Ph)_4(\mu\text{-}\eta^{12}\text{-arene})]$ and $[(Me_2\text{-cAAC})_2Hf(X)_2]$ (X = Cl, CH_2Ph).[9] Hence, a new class of hafnium(IV) complexes with a dianionic naphthalene or anthracene ligand may open up an alternative route to explore the chemistry of reduced Hf complexes. Herein we report a series of hafnium complexes with reduced naphthalene and anthracene ligands supported by the aryl-substituted triamidoamine ligand ({(3,5-$Me_2C_6H_3$)NCH_2CH_2}$_3N^{3-}$).[10] The strong reducing nature of these reduced arene complexes was shown by the reduction of benzonitrile and azobenzene, and the high basicity of the reduced arene ligands was demonstrated by the reaction with weak Brønsted acids, such as *tert*-butylacetylene.

Results and Discussion

Synthesis and Structure of Reduced Arene Complexes

The starting material [HfCl(Xy-N_3N)(thf)] (**1-Cl**; Xy-N_3N = {(3,5-$Me_2C_6H_3$)NCH_2CH_2}$_3N^{3-}$) was prepared from H_3(Xy−N_3N) and $[Hf(NMe_2)_4]$, following a similar method used for [TiCl(Xy−N_3N)].[11] In the first step, a mixture of H_3(Xy−N_3N) and $[Hf(NMe_2)_4]$ was stirred in toluene for 30 min at room temperature to obtain [Hf(NMe_2)(Xy−N_3N)] (**1-NMe_2**), which after work-up was isolated as a colorless solid in 82 % yield (see Supporting Information (SI), Sec. 2.1). Protonation of **1-NMe_2** with $[NEt_3H]Cl$ in THF under ambient condition afforded the chlorido complex **1-Cl** as a colorless solid in 96 % yield (see SI, Sec. 2.2). When the protonation was carried out in CH_2Cl_2, the chlorido complex [HfCl(Xy−N_3N)(NMe_2H)] was formed as a NMe_2H adduct.[12] The higher coordination number for the hafnium chlorido

[*] Dr. P. Ghana, S. Schrader, Dr. T. P. Spaniol, Prof. U. Englert, Prof. J. Okuda
Institute of Inorganic Chemistry, RWTH Aachen University
Landoltweg 1, 52056 Aachen (Germany)
E-mail: jun.okuda@ac.rwth-aachen.de
Dr. T. Rajeshkumar, Prof. L. Maron
Université de Toulouse et CNRS
INSA, UPS, UMR 5215, LPCNO
135 Avenue de Rangueil, F-31077 Toulouse (France)
E-mail: laurent.maron@irsamc.ups-tlse.fr
Supporting information and the ORCID identification number(s) for the author(s) of this article can be found under: https://doi.org/10.1002/anie.202103755.

complex compared to the corresponding titanium complex can be explained with the larger size of the hafnium ion. Both starting materials were fully characterized by multinuclear NMR spectroscopy and elemental analysis. In addition, the octahedral geometry of the hafnium center in **1-Cl** was confirmed by single-crystal X-ray diffraction (see SI, Figure S29). Compound **1-Cl** is the first example of a structurally characterized triamidoamine ligand-supported hafnium chloride.

Reduction of **1-Cl** with two equivalents of potassium naphthalenide (Knaph) or anthracenide (Kanth) under an atmosphere of nitrogen or argon led to a distinct color change from colorless to dark brown (for Knaph) or dark red (for Kanth). ^{1}H NMR spectroscopy revealed the selective formation of the reduced arene complexes [K(thf)][Hf(Xy−N_3N)(naph)] (**2-naph**) or [K(thf)][Hf(Xy−N_3N)(anth)] (**2-anth**) along with one equivalent of free arene (Scheme 1). After work-up, the reduced arene complexes were isolated as bright brown and dark red solids in 82 and 91 % yield, respectively (see SI, Sec. 2.3 and 2.4). Unlike the previously reported scandium naphthalene complex [K(thf)$_2$][Sc{N(*t*Bu)(Xy)}$_2$(naph)], **2-naph** does not reduce anthracene to form the corresponding reduced anthracene complex **2-anth**, indicating a lower reduction potential of **2-naph** as compared to that of the scandium complex.[4i] While **2-anth** is a thermally stable solid, compound **2-naph** decomposes slowly both in solution and in the solid state when stored at room temperature. However, **2-naph** can be stored for several months at −40 °C under argon atmosphere. The arene complexes are highly soluble in THF and DME, moderately soluble in Et_2O and aromatic solvents, and insoluble in aliphatic solvents.

The reduction of **1-Cl** resulted in a quite different outcome when compared to that of the analogous titanium(IV) complex [TiCl(Xy-N_3N)]. Whilst the reduction of [TiCl(Xy−N_3N)] with two equivalents of potassium metal or potassium naphthalenide under dinitrogen afforded a stable titanium dinitrogen complex K$_2$[{Ti(Xy−N_3N)}$_2$(μ_2-N_2)],[11] the reduction of **1-Cl** with potassium naphthalenide under dinitrogen atmosphere produced the reduced naphthalene hafnium complex instead of a dinitrogen complex K$_2$[{Hf(Xy−N_3N)}$_2$(μ_2-N_2)]. Such a difference in the outcome of the reduction of [MCl(Xy−N_3N)(thf)$_n$] (M = Ti, n = 0; M = Hf, n = 1) is most likely due to the reluctance of hafnium to form complexes with low-valent hafnium that is required to activate dinitrogen.[13]

Treatment of the reduced arene complexes **2-naph** and **2-anth** with one equivalent of 18-crown-6 in THF led to the corresponding crown ether complexes [K(18-crown-6)][Hf(Xy−N_3N)(naph)] (**2-naph-C**) and [K(18-crown-6)][Hf(Xy−N_3N)(anth)] (**2-anth-C**, Scheme 1), which were isolated in high yield as dark green and orange solids, respectively (see SI, Sec. 2.4 and 2.6). These crown ether complexes are thermally more stable than their corresponding crown ether-free analogues.

The reduced arene complexes were characterized by multinuclear NMR spectroscopy and elemental analysis. In addition, the solid-state structure of **2-anth-C** was confirmed by single-crystal X-ray diffraction (Figure 1). Several attempts to obtain crystal structures of other reduced arene complexes remained unsuccessful due to the instability of the crystals which seem to lose co-crystallized solvent molecules very fast. The molecular structure of **2-anth-C** revealed a separated ion pair with the potassium cation located in a pocket formed by the 18-crown-6 and two THF molecules. The dianionic anthracene ligand binds the hafnium center in a σ^2,π-coordination fashion with Hf1−C1/C4 and Hf1−C2/C3 distances of 2.500(9)/2.474(9) Å and 2.455(9)/2.445(10) Å, respectively. The Hf1−C1/C4 bonds are marginally longer than the Hf1−C2/C3 bonds. This bonding pattern differs from those of the previously known reduced arene complexes with a σ^2,π-coordination, where the σ-bonds are shorter than the π-bonds.[4i] However, the alternating bond lengths of C1−C2 (1.442(14) Å), C2−C3 (1.376(14) Å) and C3−C4 (1.457(13) Å), as well as a large folding angle of 40.6(8)° between the planes defined by C1-C2-C3-C4 and C1-C9A-C4A-C4 indicate rather a σ^2,π-coordination of the reduced anthracene ligand than a π^2-canonical structure. The Hf−C_{anth} bond lengths (d(Hf−C_{anth})$_{avg}$ = 2.4685 Å) in **2-anth-C** compare very well with that of the only known homoleptic hafnium-reduced anthracene complex [K(18-crown-6)]$_2$[Hf($C_{14}H_{10}$)$_3$] (d(Hf−C_{anth})$_{avg}$ = 2.467 Å).[8] As expected, the triamidoamine ligand binds the hafnium center in a trigonal monopyramidal geometry with the hafnium center residing 0.672(5) Å above the equatorial plane formed by the three amido nitrogen atoms.

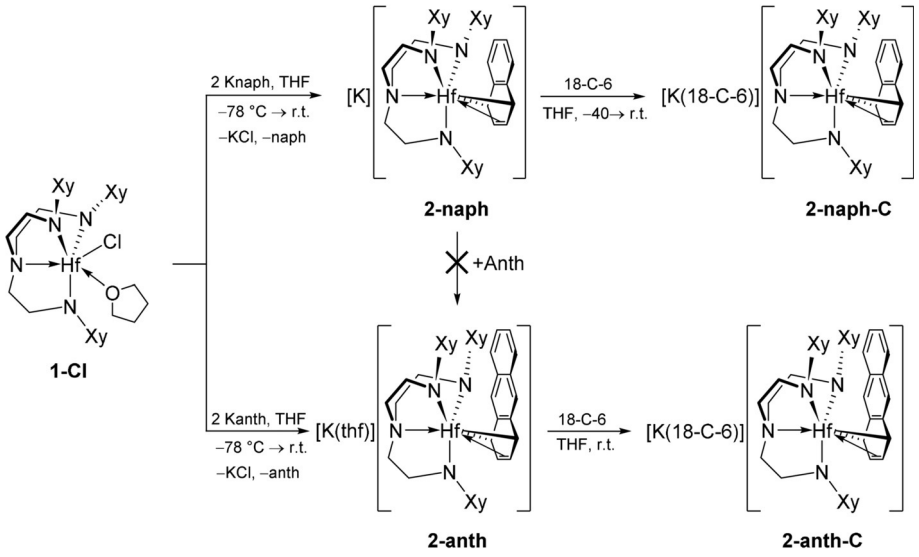

Scheme 1. Synthesis of the hafnium-reduced arene complexes; Xy = 3,5-$Me_2C_6H_3$.

Further structural information of the reduced arene complexes **2-naph**/**2-naph-C** and **2-anth**/**2-anth-C** in solution is provided by ^{1}H and ^{13}C{^{1}H} NMR spectroscopy. In contrast to the pseudo C_s-symmetric

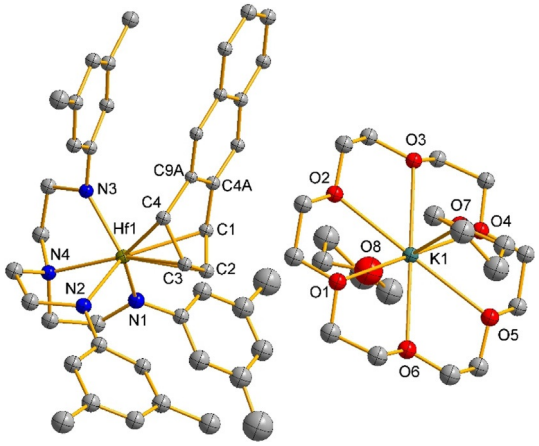

Figure 1. Molecular structure of compound **2-anth-C** in the crystal lattice of **2-anth-C**·$(thf)_2$ in the solid state with displacement parameters at 30% probability level.[22] Hydrogen atoms are omitted for clarity. Selected interatomic distances (Å)and angles (°): Hf1-N1 2.114(9), Hf1-N2 2.133(9), Hf1-N3 2.191(9), Hf1-N4 2.358(9), Hf1-C1 2.500(9), Hf1-C2 2.455(9), Hf1-C3 2.445(10), Hf1-C4 2.474(9), C1-C2 1.442(14), C2-C3 1.376(14), C3-C4 1.457(13), C4-C4A 1.483(12), C4A-C9A 1.432-(13), C1-C9A 1.446(12); N1-Hf1-N2 116.9(3), N1-Hf1-N3 113.0(3), N2-Hf1-N3 101.5(3), N1-Hf1-N4 71.6(3), N2-Hf1-N4 72.4(3), N3-Hf1-N4 71.0(3).

structure in the solid state, a single set of signals for the triamidoamine ligand shows an overall C_{3v}-symmetric structure in [D_8]THF or [D_6]benzene (see SI, Figure S6–S13). This higher symmetry is not the only proof of a fluxional process on the NMR time scale. An addition of free anthracene to the anthracene complexes leads to very broad signals in the ^{1}H NMR spectrum due to the fast exchange with the reduced anthracene ligand. A similar fluxional behavior was also observed for a reduced naphthalene complex of zirconium with a similar tetradentate, trianionic [O_3C] ligand.[7b] The most characteristic signals in the ^{1}H NMR spectra are those of the reduced naphthalene and anthracene ligands which appear markedly upfield shifted compared to those in the free ligands. For example, the ^{1}H NMR spectrum of **2-naph** displays four multiplets for the naphthalene ligand at $\delta = 2.60$ ($C^{1,4}$-*H*), 5.02 ($C^{2,3}$-*H*), 5.30 ($C^{5,8}$-*H*) and 5.82 ppm ($C^{6,7}$-*H*) (Figure S6), which appear at significantly higher field than in free naphthalene ($\delta = 7.45$ and 7.84 ppm, in [D_8]THF). Similarly, **2-anth** shows five upfield shifted signals for the reduced anthracene ligand at $\delta = 2.63$ ($C^{1,4}$-*H*), 4.96 ($C^{2,3}$-*H*), 5.06 ($C^{9,10}$-*H*), 6.48 ($C^{5,8}$-*H*) and 6.55 ppm ($C^{6,7}$-*H*) (Figure S10). The most upfield shifted multiplet at $\delta = 2.63$ for **2-anth** also confirms that the anthracene ligand coordinates via its terminal and not by its central ring, because in this case the $C^{9,10}$-*H* singlet signal should be most upfield shifted. The same coordination behavior in solution even at elevated temperature is shown by ^{1}H NMR spectra between 298 K and 363 K, which do not show any significant alteration of the signal pattern of the anthracene ligand (Figure S14), except a broadening of some signals at higher temperature.

In order to rationalize the coordination mode of the anthracene ligand in **2-Anth-C**, DFT calculations (B3PW91 functional) were carried out.[14] In particular, the energy difference between the 1,4- vs. the 9,10-coordination of the anthracene dianion was investigated. First of all, the two coordination modes were found to be possible with a preference of 12.0 kcal mol^{-1} for the 1,4-coordination in line with the experimental observation. The HOMO of the complex clearly describes the Hf–anthracene σ interaction (Figure 2). At the Natural Bonding Orbital level, two Hf–C σ bonds are

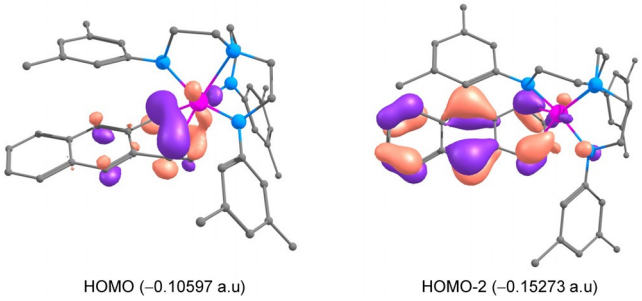

Figure 2. DFT-computed HOMO and HOMO−2 orbitals of **2-Anth-C** (1,4-coordination). Hydrogen atoms and the counter cation are omitted for clarity. Color code: pink (Hf), gray (C), blue (N), orange (positive density), violet (negative density).

found and appear to be strongly polarized toward C (82.5%) in line with a pronounced ionic interaction. This explains the low Wiberg Bond Indexes (ca. 0.1) for the Hf–C bonds. At the second-order donor–acceptor Natural Bonding Orbital (NBO) analysis, donation from the C_2–C_3 π bond is also found (roughly 60 kcal mol^{-1}), in line with a σ^2,π-coordination mode. For the 9,10-coordination mode, the bonding analysis is quite similar (WBI of 0.1) but the Hf–C bonds are found to be purely of donor–acceptor type and therefore weaker, explaining the lower stability of this coordination mode.

Reaction with Benzonitrile

The strong reducing nature of the anthracene complexes was exploited in the C–C coupling reaction between organonitriles and the anthracene ligand. Addition of an excess of benzonitrile to a THF solution of **2-anth** at −36 °C led to a rapid color change from bright red to greenish brown. Monitoring the reaction mixture by ^{1}H NMR spectroscopy revealed an immediate formation of the unusual bis(iminyl) complex [K(thf)][Hf(anth)(Xy–N_3N)(PhC=N)$_2$] (**3**) as the result of insertion of two equivalents of benzonitrile into the Hf–C_{anth} bonds (Scheme 2). Compound **3** was isolated as thermolabile, red crystals after diffusion of *n*-pentane into a concentrated THF solution of a mixture of **2-anth** and benzonitrile at −36 °C (see SI, Sec. 2.7). Compound **3** is moderately soluble in THF, sparingly soluble in aromatic solvents and insoluble in aliphatic solvents.

The solid-state structure of **3** was established by single-crystal X-ray diffraction and reveals that the C–C coupling reaction proceeds through the C9/C10 atoms of the anthracene ligand, although it is coordinated to the hafnium center through its terminal ring. The molecule crystallizes as a contact ion pair with the potassium cation located in

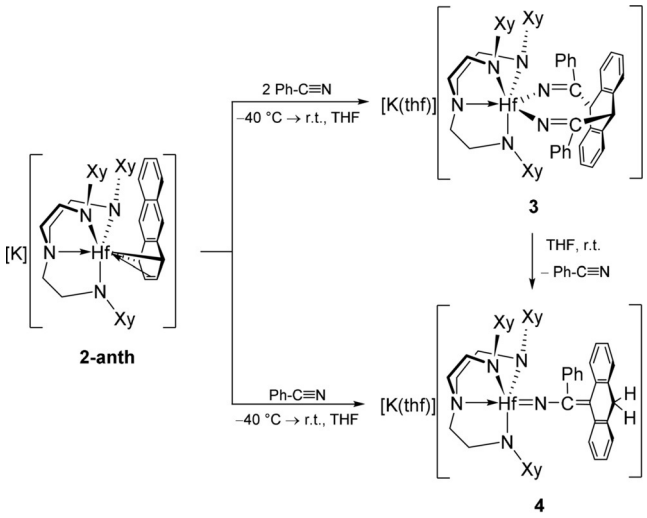

Scheme 2. Reduction of benzonitrile with the hafnium-reduced anthracene complex.

a pocket formed by three THF molecules (d(K1−O)$_{avg}$ = 2.73 Å), one iminyl ligand (d(K1−N1) = 3.085(5) Å), one amido ligand (d(K1−N3) = 2.947(4) Å), and aromatic rings of triamidoamine and anthracene ligands (d(K1−C)$_{avg}$ = 3.19 Å) (Figure 3). In the C_1-symmetric structure, the hafnium center resides in a distorted octahedral environment formed by the triamidoamine and diiminyl anthracene ligands. The three amido groups bind to the hafnium center in a meridional fashion with the bite angle varying between 85.04(18) and 89.87(17)°. The equatorial Hf−N$_{iminyl}$ bond (d(Hf1−N1) = 2.167(4) Å) is much longer than that of the axial Hf−N$_{iminyl}$ bond (d(Hf1−N2) = 2.075(4) Å), most likely due to the stronger *trans*-influence of the amide ligand compared to

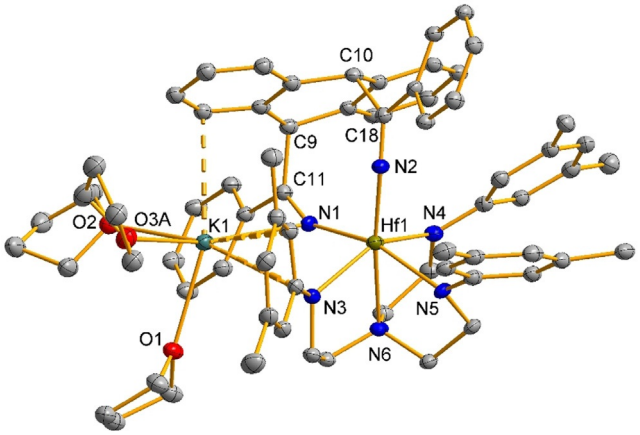

Figure 3. Molecular structure of compound **3** in the crystal lattice of **3**·2(THF) in the solid state with displacement parameters at 20% probability level.[22] Hydrogen atoms are omitted for clarity. Selected interatomic distances (Å) and angles (°): Hf1-N1 2.167(4), Hf1-N2 2.075(4), Hf1-N3 2.206(4), Hf1-N4 2.157(5), Hf1-N5 2.211(4), Hf1-N6 2.366(4), C11-N1 1.245(7), C18-N2 1.235(7), C9-C11 1.575(7), C10-C18 1.564(7), K1-N1 3.085(5), K1-N3 2.947(4); N1-Hf1-N5 158.47(17), N2-Hf1-N6 173.94(17), N3-Hf1-N4 146.85(17), N1-Hf1-N2 99.75(16), Hf1-N1-C11 153.4(4), Hf1-N2-C18 158.4(4).

the amine ligand. However, the equatorial Hf−N$_{iminyl}$ single bond length compares well with the other Hf−N$_{amide}$ single bond lengths (d(Hf1−N$_{amide}$)$_{avg}$ = 2.191 Å). The nearly identical C=N double bond lengths of the iminyl groups (d(C11−N1) = 1.245(7) Å and d(C18−N2) = 1.235(7) Å) compare well with the C=N bond lengths in our recently reported mono-(iminyl) anthracene complexes of scandium [Li(thf)$_n$][Sc{N-(*t*Bu)Xy}$_2$(anth)(R−C=N)] (R = C$_6$H$_4$-4-OMe (d(C−N) = 1.259(5) Å), *t*Bu (d(C−N) = 1.264(4) Å); n = 0–2).[4i] The anthracene ligand in **3** is more flat than that in the precursor **2-anth-C**, as evident from the folding angle of 13.3(4)° (**3**) vs. 40.6(8)° (**2-anth-C**). To the best of our knowledge, such a double C−C coupling reaction of reduced nitrile groups by a reduced anthracene complex is unprecedented. The reduction of organonitriles with alkali metals or with reduced arene complexes of alkali metals commonly leads to the decyanation of the nitriles and C−C coupling reactions of the reduced nitrile groups are a rarely observed pathway.[4i,15] However, C−C coupling between two organonitriles at group 4 metal centers is a well-known reaction.[16]

In contrast to the C_1-symmetric structure in the solid state, the ^{1}H and ^{13}C NMR spectra of compound **3** in [D$_8$]THF reveal an overall more symmetric (C_s) structure in solution, as evident from the two set of signals in a 2:1 ratio for the triamidoamine ligand (Figure S16 and S17). The most notable signals in the ^{1}H NMR spectrum of **3** are those of the benzylic group (C^{9,10}-*H*) of the anthracene ligand at δ = 6.24 and 6.47 ppm, which appear at significantly low field despite of their sp^3-hybridization. In fact, these signals appear at even lower field than those in our recently reported scandium iminyl anthracene complex [Li][Sc{N(*t*Bu)Xy}$_2$(anth)(R−C=N)] (R = C$_6$H$_4$-4-OMe; δ(C^{10}-*H*) = 5.68 ppm).[4i] In the ^{13}C NMR spectrum, the most characteristic signals are those of the iminyl groups (Ph*C*=N$^-$) at δ = 167.0 and 176.0 ppm.

Monitoring the decomposition of **3** in [D$_8$]THF by ^{1}H NMR spectroscopy revealed that the diiminyl anthracene complex selectively loses one equivalent of benzonitrile to form the hafnium imido complex [K(thf)][Hf(anth)(Xy−N$_3$N)(PhCN)] (**4**) after migration of a proton from C9 to C10 carbon atom of the anthracene ligand (Scheme 2). In fact, stirring a greenish brown solution of **2-anth** and 1 equivalent of benzonitrile at room temperature for 48 h led to the selective formation of **4**, which was isolated after work-up as an analytically pure, orange solid in 61% yield (see SI, Sec. 2.8). Unlike **3**, compound **4** is thermally stable, but decomposes quickly upon exposure to air. The reason behind the extrusion of one benzonitrile from **3** to form compound **4** is not known yet, but most likely is due to the steric congestion around the hafnium center in **3**.

Compound **4** was characterized by multinuclear NMR spectroscopy and elemental analysis. The molecular structure was confirmed by single-crystal X-ray diffraction, which reveals a contact ion pair with the potassium cation located between two molecular fragments through the coordination with one imido nitrogen atom and three xylyl groups of the two triamidoamine ligands and forms a polymeric structure in the solid state (Figure 4 and Figure S30). The hafnium center adopts a distorted trigonal bipyramidal coordination geometry, with the imido and the amine nitrogens occupying the

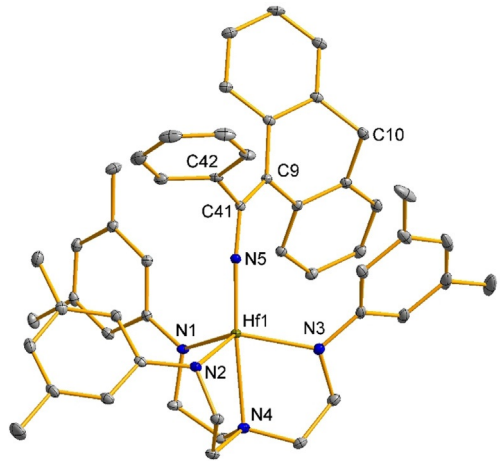

Figure 4. Molecular structure of the anion of compound **4** in the crystal lattice of **4**·(C_6H_6) in the solid state with displacement parameters at 30% probability level.[22] Hydrogen atoms are omitted for clarity. Selected interatomic distances (Å) and angles (°): Hf1-N1 2.1682(16), Hf1-N2 2.1710(17), Hf1-N3 2.1375(17), Hf1-N4 2.4137-(17), Hf1-N5 1.9093(17), N5-C41 1.345(2), C9-C41 1.377(3); N1-Hf1-N2 104.05(6), N2-Hf1-N3 117.72(6), N1-Hf1-N3 111.18(5), N1-Hf1-N4 76.91(6), N2-Hf1-N4 75.70(6), N3-Hf1-N4 74.32(6), N4-Hf1-N5 175.60(6), Hf1-N5-C41 167.88(14), N5-C41-C9 124.73(18), N5-C41-C42 113.35(16), C9-C41-C42 121.84(18).

two apical positions (∡N4-Hf1-N5 = 175.60(6)°), leaving the other three amide nitrogens on the equatorial plane. The Hf1–N5 double bond of 1.9093(17) Å is significantly shorter (11.6%) than the Hf1–N_{amide} bonds (d(Hf1–N_{amide})$_{avg}$ = 2.1589 Å), but compares well with the reported Hf–N bonds in the hafnium imido complexes (d(Hf1–N_{imido})$_{avg}$ = 1.963 Å).[17] The anthracene group is bonded to the benzonitrile group through a double bond as evident from the C9–C41 bond length of 1.377(3) and the planarity around C9 (Σ∡C9 = 359.89°) and C41 (Σ∡C41 = 359.92°) atoms.

The ^{1}H and ^{13}C NMR spectroscopic studies provide further structural information of **4** in solution. In contrast to the C_1-symmetric structure in the solid state, compound **4** displays a time-averaged C_3-symmetry in [D_8]THF at 298 K, as indicated by a single set of signals for the triamidoamine ligand (Figure S18). The most characteristic signal in the ^{1}H NMR spectrum is that of the CH_2 proton of the anthracene group at δ = 3.34 ppm that appears markedly upfield shifted compared to that of the C^9/C^{10}-*H* of **3** (δ = 6.24 and 6.47 ppm). In the ^{13}C NMR spectrum, the signals for the doubly bonded carbon atoms C9 and C41 appear at δ = 116.1 and 160.0 ppm, respectively. These spectroscopic features fully support the solid-state structure observed by single-crystal X-ray diffraction.

DFT calculations were carried out to understand the reaction mechanism for the reaction of **2-anth** with benzonitrile (Figure 5). The reaction begins with the coordination of benzonitrile to the Hf center, which is slightly endothermic (3.1 kcal mol^{-1}) and forms the intermediate **Int1**. The endothermic reaction is explained by the fact that the coordination of benzonitrile induces the switch from 1,4- to 3,4-coordination of the anthracene ligand to the hafnium center. From **Int1**, two possible insertions can occur either at C1 or at C10. Both were calculated and the insertion at C10 is preferred by 8.6 kcal mol^{-1} (see **TS1** and **TS1′** in Figure 5). The insertion barrier is 5.1 kcal mol^{-1} (only 2.0 kcal mol^{-1} from **Int1**), in line with a kinetically facile reaction. The height of the barrier is easily explained by the fact that the ring slippage induced by the benzonitrile coordination implies a delocalization of the C1 lone pair and especially at the C10 position. Following the Intrinsic Reaction Coordinate it yields the merely stable (−1.2 kcal mol^{-1} with respect to the entrance channel) intermediate **Int2**, with a 3,10-coordination. For similar reasons as described above, a second benzonitrile insertion can occur at the C9 position after the favorable coordination of PhCN (**Int4**, −8.1 kcal mol^{-1}). The associated barrier is 3.9 kcal mol^{-1}, indicating a fast reaction. This yields the formation of complex **3** that is thermodynamically stable (−15.9 kcal mol^{-1}). In the absence of a second molecule of benzonitrile, **Int2** can isomerize to form a more stable complex. Indeed, a direct 1,4-hydrogen shift (from C9 to C10) with an accessible barrier of 18.8 kcal mol^{-1}, yields

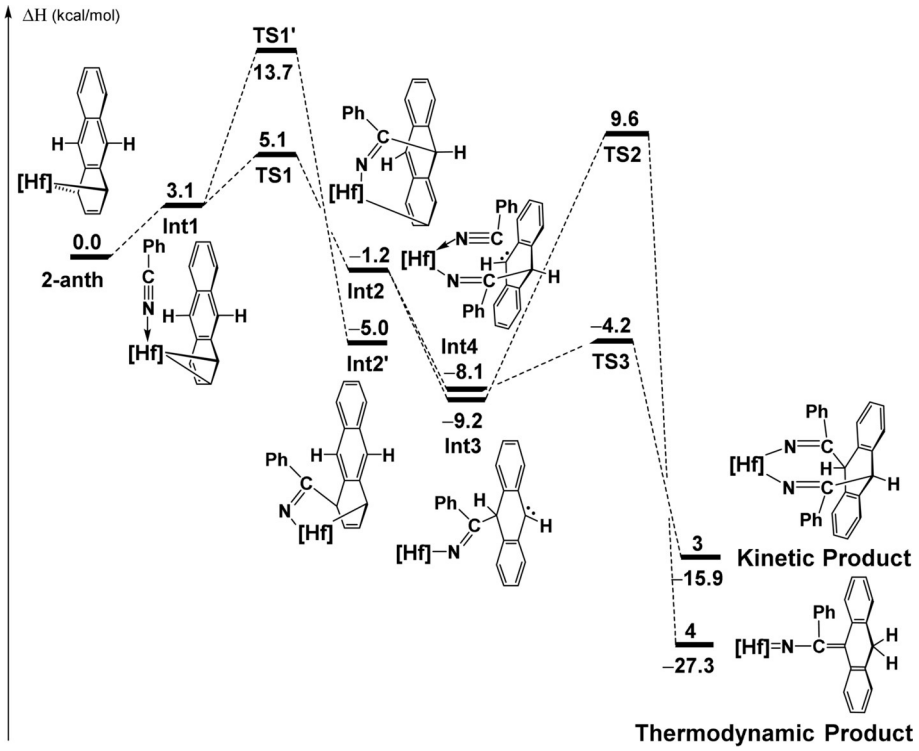

Figure 5. Calculated enthalpy profile for the reaction of **2-anth** with PhCN at room temperature. In the profile, [Hf] represents [K(thf)][Hf(Xy–N_3N)]; formal charges are omitted for clarity.

complex **4** that is the most stable complex (−27.3 kcal mol^{-1}). Therefore, one can conclude that complex **3** is formed under kinetic control, whereas complex **4** is the thermodynamic product.

Reaction with Azobenzene

The reducing as well as the labile nature of the anthracene ligand in **2-anth** were further explored in the reduction of azobenzene. Treatment of **2-anth** with one equivalent of azobenzene led to the diphenylhydrazido(2−) complex [K][Hf(η^2-PhNNPh)(Xy−N_3N)] (**5**) after elimination of anthracene. In this reaction, the dianionic anthracenyl group acts as a two-electron donor ligand. Compound **5** was isolated as an analytically pure, yellow powder in 77% yield (see SI, Sec. 2.9). Although diphenylhydrazido(2−) complexes of the group 4 metals Ti and Zr are known,[18] a corresponding hafnium analogue remained elusive and compound **5** represents the first example of a structurally characterized hafnium diphenylhydrazido(2−) complex. As a solid it is thermally stable, but decomposes instantaneously upon exposure to air.

Single-crystal X-ray diffraction of compound **5** reveals a contact ion pair with the potassium cation bonded to three THF molecules, one amide nitrogen of azobenzene and two xylyl groups of the triamidoamine ligand (Figure 6). The six-coordinate hafnium center adopts a distorted trigonal prismatic geometry. The phenyl groups of the azobenzene ligand are oriented in a staggered conformation, as evident from the C_{Ph}-N1-N2-C_{Ph} torsion angle of −82.6(4)°. The dianionic nature of the azobenzene ligand is evident from the elongated N−N bond (d(N1−N2) = 1.463(4) Å) in **5** compared to free azobenzene (d(N−N) = 1.249(4) Å).[19] In addition, the short Hf1−N1 and Hf1−N2 bond lengths of 2.190(3) and 2.082(3) Å, respectively, compare better with the other Hf−N_{amide} bond lengths (d(Hf1−N_{amide})$_{avg}$ = 2.147 Å) than the Hf1−N_{amine} bond length of 2.347(3) Å in compound **5**.

Compound **5** was further characterized by multinuclear NMR spectroscopy and its composition was confirmed by elemental analysis. The ^{1}H and ^{13}C NMR spectra in [D_8]THF display a single set of signals for the xylyl groups and the azobenzene ligand, indicating a C_3-symmetric structure in solution. The higher symmetry in solution compared to the *pseudo* C_s-symmetric structure in the solid state can be rationalized with a fluxional process on the NMR time scale, which is also evident from the broadening of several signals both in the ^{1}H and ^{13}C NMR spectra (Figure S21 and S22).

Group 4 metal hydrazido(2−) complexes are known to react with alkynes via two different pathways, depending on the type of alkynes.[18a,c] While terminal alkynes with a weakly acidic proton preferably protonate one of the amide groups of the hydrazido(2−) ligand to form a hydrazido(1−) complex, internal alkynes undergo cycloaddition to form metallacycles. When compound **5** was treated with one equivalent of terminal alkyne such as phenylacetylene, selective formation of the hydrazido(1−) complex [K][Hf(PhNN(H)Ph)(Xy−N_3N)(C≡CPh)] (**6**) was observed at room temperature (Scheme 3). However, compound **5** does not react with internal alkynes such as diphenylacetylene or 4,4-dimethyl-2-pentyne, probably due to the steric congestion around the hafnium center. After work-up compound **6** was isolated as an analytically pure, yellow solid in 90% yield (see SI, Sec. 2.10). It is a thermally stable solid but sensitive towards air.

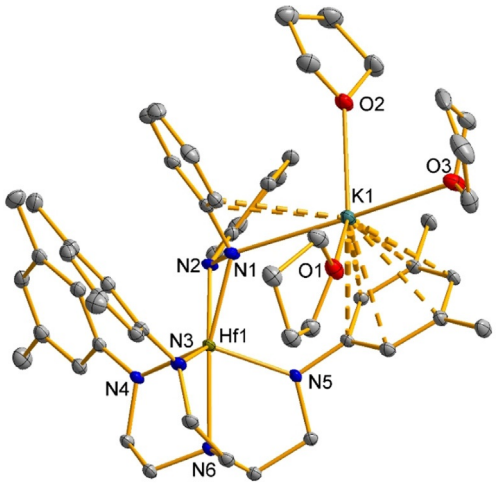

Figure 6. Molecular structure of compound **5** in the crystal lattice of **5**·3(THF) in the solid state with displacement parameters at 30% probability level.[22] Hydrogen atoms are omitted for clarity. Selected interatomic distances (Å) and angles (°): Hf1-N1 2.190(3), Hf1-N2 2.082(3), Hf1-N3 2.162(3), Hf1-N4 2.155(3), Hf1-N5 2.123(3), Hf1-N6 2.347(3), N1-N2 1.463(4), K1-O1 2.790(3), K1-O2 2.723(3), K1-O3 2.840(3), K1-N1 2.940(3); N1-Hf1-N6 158.58(10), N2-Hf1-N6 158.24(11), N1-Hf1-N2 39.96(11), N3-Hf1-N6 73.09(10), N4-Hf1-N6 74.54(10), N5-Hf1-N6 72.54(10).

Along with single-crystal X-ray diffraction, compound **6** was fully characterized by multinuclear NMR and IR spectroscopy. The composition was confirmed by elemental analysis. The crystal structure shows a disordered structure with co-crystallized solvent molecules. However, the structure confirms the expected atomic connectivity with a terminal phenyl acetylide ligand (Figure S31). Due to the disordered structure, bonding parameters were not discussed further. As expected, the ^{1}H and ^{13}C NMR spectra in [D_8]THF at room temperature confirm a C_1-symmetric structure in solution and show three sets of signals for the xylyl groups (Figure S23 and S24). The most notable signal in the ^{1}H NMR spectrum is that of the low field shifted N−*H* signal at 6.36 ppm. In the ^{13}C NMR spectrum, the signals for the triply bonded carbons

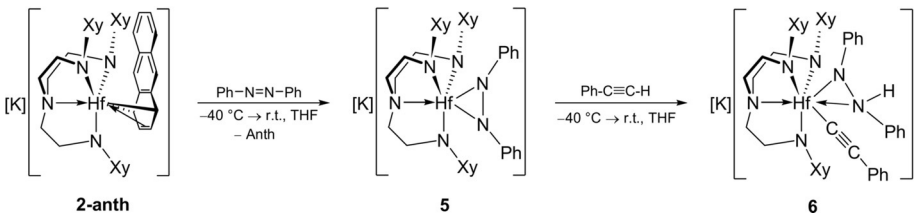

Scheme 3. Reduction of azobenzene with **2-anth** and further reaction with phenylacetylene.

of the phenyl acetylide ligand appear at 128.1 (*C*CPh) and 149.6 (*C*CPh) ppm. The IR spectrum obtained in a KBr pellet displays a weak signal at 3214 cm^{-1}, which is characteristic for a N–H stretching vibration. The signal appears at a slightly lower wavenumber than that the corresponding N–H stretching band in a similar zirconium hydrazido(1–) complex $[(ArO)_2Zr(Me)(\eta^2\text{-NPhNHPh})]$ (ArO = 2,6-di-*tert*-butylphenoxide) which appears at 3254 cm^{-1}.[20]

Reaction with tert-Butylacetylene

Attempts to protonate the reduced anthracene ligand with $[NEt_3H]Cl$ or $[NEt_3H][BPh_4]$ led to an unselective decomposition of the anthracene complex **2-anth**. However, the protonation with a weak Brønsted acid such as *tert*-butylacetylene resulted in the selective protonation of the anthracene ligand affording the diacetylide complex $[K][Hf(C{\equiv}C\mathit{t}Bu)_2(Xy{-}N_3N)]$ (**7**) along with 9,10-dihydroanthracene (Scheme 4). Compound **7** was isolated after work-up as a light green powder in 80% yield (see SI, Sec. 2.11). Treatment of **7** with one equivalent of 18-crown-6 in THF led to the corresponding crown ether complex $[K(18\text{-crown-}6)][Hf(C{\equiv}C\mathit{t}Bu)_2(Xy{-}N_3N)]$ (**7-C**) which was isolated as green crystals

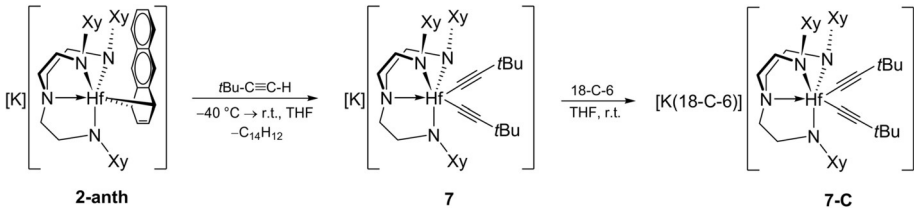

Scheme 4. Reaction of **2-anth** with the weak Brønsted acid *t*BuC≡CH.

by diffusion of *n*-hexane into a concentrated THF solution of **7-C** (see SI, Sec. 2.12). Both acetylide complexes are thermally stable solids, but decompose upon exposure to air.

The diacetylide complexes **7** and **7-C** were characterized by multinuclear NMR spectroscopy and elemental analysis. In addition, the molecular structure of **7-C** was determined by single-crystal X-ray diffraction (Figure 7). Complex **7-C** represents the first example of a structurally characterized hafnium acetylide complex outside the cyclopentadienyl ligand system.[21] In spite of the encapsulation with 18-crown-6, the potassium cation is still coordinated to a xylyl group of the triamidoamine ligand ($d(K{-}C)_{avg}$ = 3.361 Å) and forms a contact ion pair in the solid state. The hafnium center in **7-C** adopts a distorted octahedral geometry formed by the tetradentate triamidoamine ligand and two acetylide ligands. While the three amido nitrogen atoms coordinate to the hafnium center in a meridional fashion, the two acetylide ligands adopt a *cis* orientation (∡C1-Hf1-C7 = 99.5(2)°). The Hf–C distances of 2.229(7) and 2.292(7) Å to the linear acetylide ligands (∡Hf1-C1-C2 = 168.0(6)°, Hf1-C7-C8 168.1(6)°) are slightly higher than that found for terminally bound hafnium acetylide complexes (2.170(5)–2.220(1) Å).[21c,e,g] The observed elongation of the Hf–C bonds is most likely due to

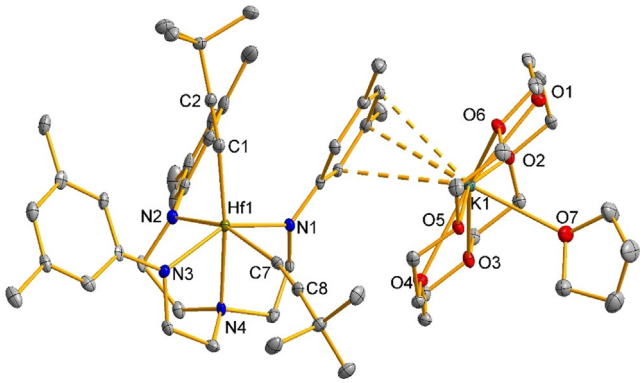

Figure 7. Molecular structure of compound **7-C** in the crystal lattice of **7-C**·(THF) in the solid state with displacement parameters at 30% probability level.[22] Hydrogen atoms are omitted for clarity. Selected interatomic distances (Å) and angles (°): Hf1-N1 2.161(5), Hf1-N2 2.199(6), Hf1-N3 2.162(5), Hf1-N4 2.405(5), Hf1-C1 2.229(7), Hf1-C7 2.292(7), C1-C2 1.213(9), C7-C8 1.214(9), K1-O1 2.845(5), K1-O2 2.814(5), K1-O3 2.821(5), K1-O4 2.779(5), K1-O5 2.857(5), K1-O6 2.757(5), K1-O7 (2.794(6); N1-Hf1-N2 88.5(2), N2-Hf1-N3 87.0(2), N3-Hf1-C7 84.3(2), N1-Hf1-C7 89.2(2), N1-Hf1-C1 106.8(2), N2-Hf1-C1 99.4(2), N3-Hf1-C1 106.8(2), C1-Hf1-C7 99.5(2), N1-Hf1-N4 75.35(19), N2-Hf1-N4 73.08(19), N3-Hf1-N4 71.51(19), C7-Hf1-N4 87.9(2), Hf1-C1-C2 168.0(6), Hf1-C7-C8 168.1(6).

the strong *trans* influence of the amine and amido ligands. The short C≡C triple bond lengths (d(C1–C2) = 1.213(9) Å, d(C7–C8) = 1.214(9) Å) of the acetylide ligands are in the expected range for a C≡C triple bond. As expected, the average $Hf{-}N_{amido}$ bond (2.174 Å) is much shorter than the $Hf{-}N_{amine}$ bond (2.405(5) Å).

In contrast to the C_1-symmetric structure in the solid state, the ^1H and ^{13}C NMR spectra of **7** and **7-C** in $[D_8]$THF at room temperature display a single set of signals both for the triamidoamine and two acetylide ligands, pointing towards a C_{3v}-symmetric structure in solution. Such a higher symmetry of **7** and **7-C** suggests a fluxional process on the NMR time scale. Apart from the expected signals for the triamido amine ligand, the ^1H NMR spectra of **7** and **7-C** show a singlet at 1.07 and 1.11 ppm, respectively, corresponding to the 18 protons for the *tert*-butyl groups of the acetylide ligands. The most characteristic signals of **7** and **7-C** in the ^{13}C NMR spectrum are those of the sp-hybridized carbon of the acetylide ligands at 119.0 and 115.1 ppm for the C^β carbon atoms, and 146.6 and 151.9 ppm for the C^α carbon atoms, respectively.

Conclusion

We have shown that the triamidoamine supported hafnium(IV)-chloride can be selectively reduced to give a series of hafnium naphthalene and anthracene complexes. These complexes can be viewed as $[HfX_5]^-$-type "ate" complexes of hafnium with the formal oxidation state of

+ IV. The reactivity studies of these reduced arene complexes towards unsaturated organic substrates such as organonitriles, azobenzene and terminal alkynes showed some similarity to the reactivity of divalent hafnium complexes. Reactions generally occur at the 9,10-carbon atoms of the anthracene-diyl ligand despite its coordination through 1,4-carbon atoms. This was rationalized using DFT calculations as being due to the low energy difference between the two isomers and high delocalization of the π-electron density within the anthracene-diyl ligand.

Acknowledgements

We thank the Deutsche Forschungsgemeinschaft for financial support, F. Ritter for assistance with X-ray crystallography and Dr. G. Fink for NMR spectroscopic measurements. Open access funding enabled and organized by Projekt DEAL.

Conflict of interest

The authors declare no conflict of interest.

Keywords: arene ligand · DFT calculation · hafnium · insertion · oxidation state

[1] E. Ellis, *Dalton Trans.* **2019**, *48*, 9538.
[2] a) R. Benken, H. Günther, *Helv. Chim. Acta* **1988**, *71*, 694; b) M. Yus, R. P. Herrera, A. Guijarro, *Tetrahedron Lett.* **2001**, *42*, 3455; c) C. Melero, A. Guijarro, M. Yus, *Dalton Trans.* **2009**, 1286; d) T. A. Scott, B. A. Ooro, D. J. Collins, M. Shatruk, A. Yakovenko, K. R. Dunbar, H.-C. Zhou, *Chem. Commun.* **2009**, 65; e) A. Uresk, N. J. O'Neil, Z. Zhou, Z. Wei, M. A. Petrukhina, *J. Organomet. Chem.* **2019**, *897*, 57.
[3] a) R. G. Lawler, C. V. Ristagno, *J. Am. Chem. Soc.* **1969**, *91*, 1534; b) W. E. Rhine, J. Davis, G. Stucky, *J. Am. Chem. Soc.* **1975**, *97*, 2079; c) B. Bogdanović, S.-T. Liao, R. Mynott, K. Schlichte, U. Westeppe, *Chem. Ber.* **1984**, *117*, 1378; d) C. L. Raston, G. Salem, *J. Chem. Soc. Chem. Commun.* **1984**, 1702; e) B. Bogdanović, N. Janke, C. Krüger, R. Mynott, K. Schlichte, U. Westeppe, *Angew. Chem. Int. Ed. Engl.* **1985**, *24*, 960; *Angew. Chem.* **1985**, *97*, 972; f) L. M. Engelhardt, S. Harvey, C. L. Raston, A. H. White, *J. Organomet. Chem.* **1988**, *341*, 39; g) M. Nir, I. O. Shapiro, R. E. Hoffman, M. Rabinovitz, *J. Chem. Soc. Perkin Trans. 2* **1996**, 1607.
[4] For selected references, see: a) E. P. Kündig, P. L. Timms, *J. Chem. Soc. Chem. Commun.* **1977**, 912; b) J. E. Ellis, D. W. Blackburn, P. Yuen, M. Jang, *J. Am. Chem. Soc.* **1993**, *115*, 11616; c) W. W. Brennessel, J. E. Ellis, M. K. Pomije, V. J. Sussman, E. Urnezius, V. G. Young, Jr., *J. Am. Chem. Soc.* **2002**, *124*, 10258; d) W. W. Brennessel, V. G. Young, J. E. Ellis, *Angew. Chem. Int. Ed.* **2006**, *45*, 7268; *Angew. Chem.* **2006**, *118*, 7426; e) J. E. Ellis, *Inorg. Chem.* **2006**, *45*, 3167; f) W. W. Brennessel, J. E. Ellis, *Inorg. Chem.* **2012**, *51*, 9076; g) W. Huang, S. I. Khan, P. L. Diaconescu, *J. Am. Chem. Soc.* **2011**, *133*, 10410; h) W. Huang, P. L. Diaconescu, *Chem. Commun.* **2012**, *48*, 2216; i) P. Ghana, A. Hoffmann, T. P. Spaniol, J. Okuda, *Chem. Eur. J.* **2020**, *26*, 10290.
[5] a) R. Wolf, E.-M. Schnöckelborg, *Chem. Commun.* **2010**, *46*, 2832; b) E.-M. Schnöckelborg, J. J. Weigand, R. Wolf, *Angew. Chem. Int. Ed.* **2011**, *50*, 6657; *Angew. Chem.* **2011**, *123*, 6787.
[6] a) E. Urnezius, W. W. Brennessel, C. J. Cramer, J. E. Ellis, P. v. R. Schleyer, *Science* **2002**, *295*, 832; b) Y. Nakanishi, Y. Ishida, H. Kawaguchi, *Dalton Trans.* **2018**, *47*, 6903.
[7] a) M. Jang, J. E. Ellis, *Angew. Chem. Int. Ed. Engl.* **1994**, *33*, 1973; *Angew. Chem.* **1994**, *106*, 2036; b) Y. Nakanishi, Y. Ishida, H. Kawaguchi, *Dalton Trans.* **2016**, *45*, 15879; c) G. T. Plundrich, H. Wadepohl, E. Clot, L. H. Gade, *Chem. Eur. J.* **2016**, *22*, 9283; d) C. H. Low, J. N. Rosenberg, M. A. Lopez, T. Agapie, *J. Am. Chem. Soc.* **2018**, *140*, 11906.
[8] R. E. Jilek, M. Jang, E. D. Smolensky, J. D. Britton, J. E. Ellis, *Angew. Chem. Int. Ed.* **2008**, *47*, 8692; *Angew. Chem.* **2008**, *120*, 8820.
[9] a) Y. Wielstra, S. Gambarotta, J. B. Roedelof, M. Y. Chiang, *Organometallics* **1988**, *7*, 2177; b) F. A. Cotton, P. A. Kibala, W. A. Wojtczak, *J. Am. Chem. Soc.* **1991**, *113*, 1462; c) D. J. Sikora, K. J. Moriarty, M. D. Rausch, A. R. Bulls, J. E. Bercaw, V. D. Patel, A. J. Carty, *Inorg. Syn.* **2007**, *28*, 248; d) Q. Liu, Q. Chen, X. Leng, Q.-H. Deng, L. Deng, *Organometallics* **2018**, *37*, 4186.
[10] a) G. E. Greco, A. I. Popa, R. R. Schrock, *Organometallics* **1998**, *17*, 5591; b) G. E. Greco, R. Schrock, *Inorg. Chem.* **2001**, *40*, 3850.
[11] P. Ghana, F. D. van Krüchten, T. P. Spaniol, J. van Leusen, P. Kögerler, J. Okuda, *Chem. Commun.* **2019**, *55*, 3231 – 3234.
[12] ^{1}H NMR spectrum of [HfCl(Xy-N$_3$N)(NMe$_2$H)] in [D$_6$]benzene (see SI, Figure S5): $\delta = 1.73$ (d, ^3J(H,H) = 6.0 Hz, 6H, N*Me*$_2$H), 1.92 (sept, ^3J(H,H) = 6.0 Hz, 1H, NMe$_2$*H*), 2.34 (s, 18H, C$_6$H$_3$-(C*H*$_3$)$_2$), 2.56 (t, ^3J(H,H) = 6.1 Hz, 6H, NC*H*$_2$), 3.62 (br t, 6H, NC*H*$_2$), 6.58 (s, 3H, *p*-C$_6$H$_3$), 7.13 ppm (s, 6H, *o*-C$_6$H$_3$).
[13] a) T. Beweries, V. V. Burlakov, M. A. Bach, S. Peitz, P. Arndt, W. Baumann, A. Spannenberg, U. Rosenthal, B. Pathak, E. D. Jemmis, *Angew. Chem. Int. Ed.* **2007**, *46*, 6907; *Angew. Chem.* **2007**, *119*, 7031; b) C. Marschner, *Angew. Chem. Int. Ed.* **2007**, *46*, 6770; *Angew. Chem.* **2007**, *119*, 6892; c) S. K. Ritter, *Chem. Eng. News* **2007**, *85*, 42.
[14] a) A. D. Becke, *J. Chem. Phys.* **1993**, *98*, 5648; b) K. Burke, J. P. Perdew, W. Yang, in *Electronic Density Functional Theory: Recent Progress and New Directions* (Eds.: J. F. Dobson, G. Vignale, M. P. Das), Plenum, New York, **1998**.
[15] J.-P. Mazaleyrat, *Can. J. Chem.* **1978**, *56*, 2731.
[16] L. Becker, P. Arndt, H. Jiao, A. Spannenberg, U. Rosenthal, *Angew. Chem. Int. Ed.* **2013**, *52*, 11396; *Angew. Chem.* **2013**, *125*, 11607; and references therein.
[17] A CSD survey (02.02.2021) gave 10 hits for complexes with Hf=N bond and with an average Hf=N bond length of 1.963 Å.
[18] a) P. J. Walsh, F. J. Hollander, R. G. Bergman, *J. Am. Chem. Soc.* **1990**, *112*, 894; b) L. D. Durfee, J. E. Hill, P. E. Fanwick, I. P. Rothwell, *Organometallics* **1990**, *9*, 75; c) P. J. Walsh, F. J. Hollander, R. G. Bergman, *J. Organomet. Chem.* **1992**, *428*, 13; d) K. Kaleta, P. Arndt, A. Spannenberg, U. Rosenthal, *Inorg. Chim. Acta* **2011**, *370*, 187; e) Z. W. Gilbert, R. J. Hue, I. A. Tonks, *Nat. Chem.* **2016**, *8*, 63.
[19] J. Harada, K. Ogawa, S. Tomoda, *Acta Crystallogr. Sect. B* **1997**, *53*, 662.
[20] C. H. Zambrano, P. E. Fanwick, I. P. Rothwell, *Organometallics* **1994**, *13*, 1174.
[21] a) M. Albrecht, G. Erker, M. Nolte, C. Krüger, *J. Organomet. Chem.* **1992**, *427*, C21; b) H. Lang, M. Herres, L. Zsolnai, *Bull. Chem. Soc. Jpn.* **1993**, *66*, 429; c) H. Lang, M. Herres, W. Imhof, *J. Organomet. Chem.* **1994**, *465*, 283; d) D. Röttger, G. Erker, R. Fröhlich, S. Kotila, *Chem. Ber.* **1996**, *129*, 1; e) S. Back, G. Rheinwald, L. Zsolnai, G. Huttner, H. Lang, *J. Organomet. Chem.* **1998**, *563*, 73; f) J. Kralik, K. Kohler, T. Ruffer, H. Lang, *Z. Naturforsch. B* **2004**, *59*, 1185; g) G. Dierker, G. Kehr, R. Fröhlich, G. Erker, S. Grimme, *Chem. Commun.* **2006**, 3912; h) V. V. Burlakov, T. Beweries, K. Kaleta, V. S. Bogdanov, P.

Arndt, W. Baumann, A. Spannenberg, V. B. Shur, U. Rosenthal, *Organometallics* **2010**, *29*, 2367.

[22] Deposition Numbers 2067640 (**2-Anth-C**·$(THF)_2$), 2067641 (**3**·$(THF)_2$), 2067642 (**4**·(C_6H_6)), 2067643 (**5**·3(THF)), and 2067645 (**7-C**·(THF)) contain the supplementary crystallographic data for this paper. These data are provided free of charge by the joint Cambridge Crystallographic Data Centre and Fachinformationszentrum Karlsruhe Access Structures service www.ccdc.cam.ac.uk/structures.

Manuscript received: March 16, 2021
Accepted manuscript online: April 23, 2021
Version of record online: May 7, 2021

